Published in final edited form as:
J Med Chem. 2009 May 14; 52(9): 2836–2845. doi:10.1021/jm801640k.

Development of novel aminoglycoside (NB54) with reduced toxicity and enhanced suppression of disease-causing premature stop mutations

Igor Nudelman[†,‡], **Annie Rebibo-Sabbah**[§,‡], **Marina Cherniavsky**[†], **Valery Belakhov**[†], **Mariana Hainrichson**[†], **Fuquan Chen**[⊥], **Jochen Schacht**[⊥], **Daniel S. Pilch**[#], **Tamar Ben-Yosef**[§], and **Timor Baasov**[†,*]

[†]The Edith and Joseph Fischer Enzyme Inhibitors Laboratory, Schulich Faculty of Chemistry, Technion-Israel Institute of Technology, Haifa 32000, Israel

[§]Department of Genetics and The Rappaport Family Institute for Research in the Medical Sciences, Faculty of Medicine, Technion - Israel Institute of Technology, Haifa 31096, Israel

[⊥]Kresge Hearing Research Institute, University of Michigan, Ann Arbor, Michigan, USA

[#]Department of Pharmacology, University of Medicine and Density of New Jersey, Robert Wood Johnson Medical School, 675 Hoes Lane, Piscataway, New Jersey 08854-5635, USA

Abstract

Nonsense mutations promote premature translational termination and represent the underlying cause of a large number of human genetic diseases. The aminoglycoside antibiotic gentamicin has the ability to allow the mammalian ribosome to read past a false-stop signal and generate full-length functional proteins. However, severe toxic side effects along with the reduced suppression efficiency at subtoxic doses limit the use of gentamicin for suppression therapy. We describe here the first systematic development of the novel aminoglycoside **2** (NB54) exhibiting superior *in vitro* readthrough efficiency to that of gentamicin in seven different DNA fragments derived from mutant genes carrying nonsense mutations representing the genetic diseases Usher syndrome, cystic fibrosis, Duchenne muscular dystrophy and Hurler syndrome. Comparative acute lethal toxicity in mice, cell toxicity and the assessment of hair cell toxicity in cochlear explants further indicated that **2** exhibits far lower toxicity than that of gentamicin.

Keywords

Aminoglycosides; Genetic Diseases; Nonsense Mutations; Translational Therapy; Cystic Fibrosis

Introduction

Many human genetic diseases including cystic fibrosis (CF), Duchenne muscular dystrophy (DMD), Usher syndrome (USH), Hurler syndrome (HS) and numerous types of cancer are caused by nonsense mutations, single point alterations in DNA that give rise to in-frame UAA, UAG or UGA codons in messenger RNA coding regions, leading to premature termination of translation and eventually to truncated, nonfunctional proteins [1]. According to the Human Gene

To whom correspondence should be addressed at: Schulich Faculty of Chemistry, Technion-Israel Institute of Technology, Haifa 32000, Israel. E-mail: chtimor@tx.technion.ac.il. Phone: (972) 48292590; Fax: (972) 48295703.
[‡]I. Nudelman and A. Rebibo-Sabbah contributed equally to this work.

Mutation Database, nonsense mutations represent about 12% of all mutations reported 2 , and for many of those diseases there is presently no effective treatment. Although gene therapy seems like a potential possible solution for genetic disorders, there are still many critical difficulties to be solved before this technique can be used in humans.

One alternative way to treat these diseases is to selectively promote translational readthrough of premature stop codons, but not of normal termination codons, so that the expression of the full-length, functional protein is restored to some extent. Some aminoglycoside antibiotics exhibit such a unique ability; they can promote readthrough of disease-causing premature stop codons in mammalian cells and partially restore the expression of functional proteins [3–7]. The aminoglycoside gentamicin can partially restore the expression of functional proteins in mouse models of DMD [8] and CF [9] carrying nonsense mutations in the dystrophin and cystic fibrosis transmembrane conductance regulator (*CFTR*) genes, respectively. Furthermore, treatment with gentamicin of patients harboring nonsense mutations in *CFTR* or dystrophin genes promoted partial production of the respective missing proteins [10–12] . These observations in conjunction with the recent indication that the enhancement of CFTR protein synthesis from <1% to as little as 5% of normal levels may greatly reduce the severity or eliminate the principal manifestations of CF disease [6, 13], point to the potential of this approach for the treatment of a large group of inherited diseases caused by nonsense mutations.

However, severe side-effects of gentamicin including renal, auditory, and vestibular toxicities [1, 7], along with the reduced readthrough efficiency at subtoxic doses in a mouse model [14] and in clinical trials [6], have limited its clinical use for this purpose. To date, nearly all suppression experiments for the potential use of aminoglycosides in the treatment of genetic diseases have been performed with commercially available drugs [5], whose high toxicity and/or low potency limit or may even preclude their use in suppression therapy in humans. Almost no efforts have been made to optimize their activity as stop codon readthrough inducers. Nevertheless, the proof-of-concept experiments with gentamicin strongly indicated that systematic search for new structures with improved termination suppression activity and lower toxicity is required to extrapolate the approach to the point where it can actually help patients [1, 7].

To address the need for such compounds, we recently developed compound **1** (also named NB30, Figure 1),[15] a new pseudo-trisaccharide derivative of the clinical aminoglycoside paromomycin. Compound **1** has significantly reduced cytotoxicity in comparison to gentamicin and paromomycin [16]. Moreover, we have recently demonstrated that **1** promotes dose-dependent suppression of nonsense mutations of the *PCDH15* gene, one of the underlying causes of type 1 Usher syndrome (USH1) [16]. However, the suppression potency of **1** was significantly lower relative to that of gentamicin and paromomycin. In attempts to further improve the suppression efficiency and reduce the toxicity of **1**, in the present work we report on the design, synthesis and comparative evaluation of the second-generation lead structure compound **2** (also named NB54, Figure 1). We show that compound **2** has significantly reduced cell, cochlear and acute toxicities, and has substantially higher stop-codon readthrough potency in both *in vitro* and *ex vivo* studies, than those of gentamicin. The data indicate that compound **2** may represent a superior choice than gentamicin in suppression therapy.

Chemistry

Design and Synthesis of the New Lead Structure Compound 2

To further improve both the premature stop codon suppression activity and toxicity of **1**, we sought to explore the effect of selective installation of the (*S*)-4-amino-2-hydroxybutanoyl (AHB) group at N-1 position to yield compound **2**, because of the following reasons. First, it has been shown that the selective introduction of an AHB group at N-1 position of several aminoglycosides is effective in lowering the acute lethal toxicity (LD_{50}) of the resulting

derivative relative to that of the parent molecule [17, 18]. For example, LD_{50} values in mg/kg of ribostamycin = 260 *vs.* butirosin (N-1-AHB-ribostamycin) = 520; neamine LD_{50} = 125 *vs.* N-1-AHB-neamine LD_{50} = 260; dibekacin LD_{50} = 71 *vs.* arbekacin (N-1-AHB-dibekacin) LD_{50} = 118. Although aminoglycosides are limited in clinical use primarily because of their oto- and nephro-toxic potential and these toxic effects are not necessarily reflected in their acute lethal toxicity, it has generally been recognized that aminoglycosides with weaker acute toxicity are prone to have less toxic potential on the renal, auditory and/or vestibular functions [17, 19]. Second, the N-1-AHB group has also significant impact on the stop-codon-readthrough potency of an aminoglycoside. For example, recent studies have indicated that the clinical doses of amikacin provide highly effective suppression of the human *CFTR*-G542X nonsense mutation in a transgenic CF mouse [14]. In contrast to amikacin, kanamycin A that differs from amikacin by only the absence of an AHB substitution at N-1 position, does not show measurable readthrough activity [5] (see also Figure S1 in Supporting Information showing comparative *in vitro* readthrough activities of amikacin and kanamycin A). Third, numerous structural and biochemical studies have revealed the impact of the flexible AHB side-chain on the improved antibacterial performance of aminoglycosides. For example, X-ray analyses of the bacterial A site in a complex with amikacin [20] and some other N-1-AHB-modified aminoglycosides [21] have demonstrated that the AHB group can increase binding affinity of aminoglycosides to the A site through making additional direct contacts. We have previously shown that **1** binds to the human cytoplasmic A site sequence ($K_a = 4.7\times10^3\ M^{-1}$) with about 100-fold weaker affinity than its parent paromomycin ($K_a = 3.9\times10^5\ M^{-1}$) [22] and exhibits about three times weaker suppression potency than paromomycin [15]. Based on these accumulative data we anticipated that the attachment of an AHB group at N-1 position of **1** could improve the binding affinity of the resulting derivative to the human cytoplasmic A site and probably improve its readthrough activity and reduce its toxicity.

The synthesis of compound **2** was accomplished in nine chemical steps from the readily available paromamine **3** as shown in Scheme 1. Regioselective differentiation of the three amino groups of paromamine **3** was achieved by employing metal-mediated chelation methodology [23]. Thus, treatment of **3** with $Zn(OAc)_2$ and Boc_2O afforded the selectively N-1-Boc-protected paromamine (40% isolated yield), which after azidation (TfN_3) gave the diazido derivative **4**. Treatment with TFA to remove the Boc group and the reaction of the resulting N-1 amine with (*S*)-2-hydroxy-4-azidobutyric acid (HOBT, DCC, Et_3N) was followed by treatment with methylamine to afford the selectively N-1-acylated product **5** in 93% yield for three steps. Regioselective acetylation of **5** with Ac_2O at low temperature gave the product **6** in 75% isolated yield. Glycosylation of **6** with the trichloroacetimidiate donor **7** [24] under the Lewis acid conditions furnished the desired pseudotrisaccharide **8** in 76% isolated yield, exclusively as a beta-anomer at the newly generated glycosidic linkage. Two sequential deprotection steps on **8**: treatment with methylamine to remove all the ester protections, and the Staudinger reaction to convert azides to the corresponding amines, afforded **2** in 78% isolated yield (for two steps).

This synthetic scheme was used to generate multigram quantities of compound **2** for various biological studies reported here. To further advance the synthesis of **2**, we have recently developed a combined chemical-enzymatic strategy for selective installation of the N-1-AHB group on various unprotected aminoglycosides by using recombinant BtrH and BtrG enzymes of butirosin biosynthesis in combination with a synthetic acyl donor [25]. Using this methodology, we quantitatively converted compound **1** to **2** in several milligrams scale by performing two enzymatic steps sequentially without purification of the intermediate products. Further investigation to scale-up the production of **2** by this methodology is currently underway.

Results

Compound 2 Induces more Effective Suppression of *PCDH15, CFTR, Dystrophin* and *IDUA* Nonsense Mutations than Gentamicin, Paromomycin and Compound 1 *in vitro*

Previous studies have shown that aminoglycosides suppress various stop codons with dramatically different efficiencies (UGA > UAG > UAA), and that the effectiveness of suppression is further dependent upon the identity of the first nucleotide immediately downstream from the stop codon (C > U > A ≥ G) and the local sequence context around the stop codon [5, 26]. Therefore, our pilot study to evaluate the readthrough efficiency of compound **2** was performed on a variety of constructs containing different sequence contexts around premature stop codons derived from the *PCDH15, CFTR, dystrophin* and *IDUA* genes that underlie USH1, CF, DMD and HS, respectively. We chose several prevalent nonsense mutations that are specific to these diseases; R3X and R245X for USH1, G542X and W1282X for CF, R3381X for DMD, Q70X and W402X for HS. DNA fragments containing the nonsense mutation or the corresponding wild type codon, in their natural context, were cloned in frame between the Renilla and the Firefly luciferase genes of the p2luc vector [26, 27]. The resulting eight nonsense mutation-carrying plasmids, including p2luc and seven disease-specific constructs, were transcribed and translated using the TNT Reticulocyte Lysate Quick Coupled Transcription/Translation System in the presence of varying concentrations of compounds **1** and **2**, gentamicin and paromomycin, and the stop codon suppression efficiency was calculated as previously reported [27] (Figure 2).

From the observed data it can be seen that all the tested aminoglycosides induced readthrough, although the efficacy was substantially different between the different constructs and the compounds tested. Of the four aminoglycosides tested, compound **2** induced the highest level of readthrough, followed by gentamicin, paromomycin and **1**. In general, UGA C tetracodon sequence showed the best translational readthrough in the presence of all four aminoglycosides tested, with UGA G and UGA A tetracodons showing lower levels of readthrough. Likewise, the UAG C tetracodon (Q70X) readthrough was less efficient than those of the parallel UGA C tetracodons (R3X and p2luc). Inhibition of translation was monitored as the ratio of Renilla luciferase activity with and without the presence of aminoglycosides. In all the eight constructs tested, the highest concentration of gentamicin and compound **2** resulted in approximately 50% reduction in overall translation, whereas the effects of paromomycin and compound **1** on translation were significantly milder resulting in approximately 40% and 30% reduction in overall translation, respectively.

Compound 2 Induces Highly Effective Suppression of the *PCDH15*-R3X Nonsense Mutation in a Mammalian Cell line

The dual luciferase reporter plasmid system that we used for the *in vitro* study described above was also employed to measure the effect of aminoglycosides on stop codon readthrough in tissue culture cells *ex vivo*. The ability of this dual luciferase reporter system to control for differences in mRNA levels between normal and nonsense-containing sequences provides a distinct advantage compared with single reporter or direct protein analysis [26, 27]. A comparative study was performed on the construct harboring the *PCDH15*-R3X nonsense mutation of USH1 in a monkey kidney cell line (COS-7) incubated with varying concentrations of **1**, **2**, gentamicin and paromomycin (Figure 3). In order to ensure over 80% cell viability for each of the tested compounds, the maximal dosage for each compound was estimated from its respective half-maximal-lethal concentration value (LC_{50} values) in COS-7 cells (Table 1). The following maximal dosages of aminoglycosides were used: gentamicin 0.25 mg/mL (0.38 mM), paromomycin 0.5 mg/mL (0.70 mM), compound **1** 1 mg/mL (1.78 mM) and compound **2** 1 mg/mL (1.53 mM).

The observed efficiency on a weight basis of aminoglycoside-induced readthrough of *PCDH15*-R3X nonsense mutation was in the order compound **2** > gentamicin ≥ paromomycin > compound **1**, a very similar trend to that observed for the suppression of the same stop mutation *in vitro* (Figure 3 and Figure 2C). Virtually the same order of readthrough efficiency was also observed for the *PCDH15*-R245X nonsense mutation suppression by this set of aminoglycosides under the same experimental conditions *ex vivo* (data not shown). Due to their relatively low cell toxicity, compounds **1** and **2** can however be used at higher dosages than gentamicin and paromomycin. Therefore, the maximal suppression levels of compounds **1** and **2** were obtained at significantly higher concentrations than those of gentamicin and paromomycin. Nevertheless, with a maximal suppression level of 5.25%, compound **2** is 1.9-fold more effective than compound **1** (2.75% suppression), 3.2-fold more effective than paromomycin (1.62% suppression), and 2.8-fold more effective than gentamicin (1.86% suppression).

Compounds 1 and 2 Exhibit Significantly Reduced Acute and Cell Toxicities than those of Gentamicin and Paromomycin

Cell toxicity of compound **2** was tested in three kidney-derived cell lines: HEK-293 (human embryonic kidney), COS-7, and MDCK (canine kidney). The measured LC_{50} values of **2** in comparison to those previously reported by us for gentamicin, paromomycin and compound **1**, under identical conditions [16] , are given in Table 1. The LC_{50} values obtained for compound **2** were 2–12 fold higher than LC_{50} values of the clinically used aminoglycosides gentamicin and paromomycin in all three cell lines tested.

It is of note that the acute lethal toxicity value (LD_{50}) reported for an aminoglycoside often differs considerably between different laboratories [17]. Such discrepancy between different reports could be explained by several factors including the strain, sex and age of the animals, the volume and rate of injection, and the pH of the aminoglycoside antibiotic solution administered to the animals [17]. To avoid such uncertainties, the comparative acute intravenous toxicity values of **1**, **2**, gentamicin and paromomycin were determined in mice under the same experimental conditions and the observed data are shown in Table 1. The observed data indicate that of the four aminoglycosides tested compound **2** is the least toxic compound. With the LD_{50} value of 500 mg/kg, **2** is approximately eight-fold less toxic than gentamicin (LD_{50} = 60 mg/kg), six-fold less toxic than paromomycin (LD_{50} = 80 mg/kg) and two-fold less toxic than compound **1** (LD_{50} = 240 mg/kg). In addition to compound **2**, compound **1** also demonstrated substantially reduced acute toxicity relative to the clinical aminoglycosides gentamicin and paromomycin. Surprisingly, the observed two-fold difference in LD_{50} values between compounds **1** and **2** is similar to that observed between ribostamycin and butirosin (LD_{50} values of 260 and 520mg/kg, respectively) [17] , suggesting that the presence of the N-1-AHB group could be responsible for the acute toxicity attenuation of compound **2** relative to that of compound **1**. These data are consistent with the earlier reported structure-toxicity relationship of various aminoglycosides [17], demonstrating that the decrease of a total charge and/or installation of N1-AHB side chain strongly impact the acute toxicity attenuation of an aminoglycoside. Furthermore, since the acute toxicity data of aminoglycosides were found to be well correlated to their neuromuscular blocking effects [28], we suggest that the reduction in the total positive charge of **2** and **1** (+4) versus that of gentamicin and paromomycin (+5), is linked to the acute toxicity attenuation due to the subsequent reduced effects on neuromuscular blocking. This suggestion is supported by earlier studies which demonstrated that the total charge of an aminoglycoside correlates with the blocking potency [29, 30], and that co-administration of Ca^{2+} antagonizes both acute toxicity and neuromuscular blocking effects induced by aminoglycosides [31].

Since both compounds **1** and **2** have the same total positive charge but differ only by the presence of an AHB side-chain, it is likely that due to the presence of a flexible AHB moiety the interaction of compound **2** with steps that control acetylcholine release at the level of presynaptic structures is less efficient than that of compound **1**. Indeed, numerous earlier studies demonstrated that aminoglycosides with the same total charge but with different structures interfere differently with the steps of calcium-mediated acetylcholine release at the level of presynaptic structures, and that this interaction is the main cause of the neuromuscular blockage induced by aminoglycosides and their subsequent toxicity [28, 32, 33].

Compounds 1 and 2 Exhibit Significantly Lower Ototoxic Potential than Gentamicin

The major irreversible side effect of aminoglycosides is ototoxicity (loss of hearing or balance), with an incidence of auditory or vestibular disturbances around 8% to 20% for a short course of therapy [34] but higher in long-term treatment, as would be needed in suppression therapy. The cellular basis of ototoxicity is the permanent destruction of hair cells in the inner ear 35. Organ cultures of the early postnatal mouse are frequently used in research on ototoxic agents and their mechanisms. The pattern of toxicity is similar to the *in vivo* action of aminoglycosides: preferential loss of outer hair cells in a base-to-apex fashion that is characteristic of aminoglycoside damage to the cochlea in both human and experimental animals [35]. The advantage of the preparation over the *in vivo* condition, however, is an accelerated time course of hair cell loss making explants an excellent model to screen for ototoxicity.

For the assessment of ototoxicity potential, compounds **1**, **2** and gentamicin were tested with cochlear explants (Figure 4A–E). Staining for F-actin revealed the organized outline of the array of three rows of outer hair cells and one row of inner hair cells in segments from the basal part of the cochlea. In the presence of 0.1 mM compound **1** (Figure 4A) or 0.1 mM compound **2** (Figure 4C) the structure of the epithelium remained normal and was indistinguishable from controls. At drug concentrations of 1 mM (Figure 4B and 4D) only few areas of outer hair cell loss (arrows) were seen and inner hair cells were normal. In contrast, hair cell loss was almost complete in the presence of 0.2 mM gentamicin (Figure 4E). Virtually the same conclusions can be drawn from an examination of the middle part and apical parts of the cochlea (Figure S2), demonstrating that both **1** and **2** have significantly lower ototoxic potential than that of gentamicin.

Compound 2 Enhances the Thermal Stability of a Human Cytoplasmic rRNA A-Site Model Oligonucleotide to a Greater Extent than Compound 1

The improved readthrough activity of **2** over that of **1** might reflect a correspondingly enhanced affinity of **2** for the eukaryotic ribosome. As a first step to assess the veracity of this hypothesis, we compared the impacts of **2** and **1** on the thermal stability of an RNA hairpin construct that models the human cytoplasmic rRNA A-site [36]. Figure 5 shows the UV melting profiles of the human cytoplasmic rRNA A-site model oligonucleotide in the absence and presence of **1** and **2** (at a [drug]/[RNA] ratio of 5). These UV melting profiles were analyzed as described in the Experimental Section to derive melting temperatures (T_m), defined as the temperature at which half the RNA molecules are single-stranded and the other half are in duplex form. Note that compound **2** binding enhances the thermal stability of the host RNA to a greater extent than compound **1** (ΔT_m = 9.7 and 4.5 °C for compounds **2** and **1**, respectively). In general, the relative extents to which ligands enhance the thermal stability of a host nucleic acid correlate with the relative affinities of the ligands for the nucleic acid [37]. Thus, our UV melting results are consistent with **2** binding the human cytoplasmic rRNA A-site with a greater affinity than **1**. It is likely that this enhanced affinity contributes, at least in part, to the observed enhanced stop codon readthrough activity of compound **2** relative to compound **1**.

Compound 2 Inhibits Prokaryotic Protein Translation with Significantly Lower Potency and Exhibits Markedly Reduced Bactericidal Activity than those of Gentamicin and Paromomycin

Recently we have shown that compound **1** is about ten-fold weaker inhibitor of prokaryotic translation than gentamicin and paromomycin [22] and exhibits almost no bactericidal activity against both Gram-negative and Gram-positive bacteria [15]. To assess whether compound **2** retains similar properties, we conducted comparative translation inhibition of **1**, **2**, gentamicin and paromomycin in a prokaryotic system, by using an *in vitro* luciferase assay (Table 1). The measured half-maximal inhibitory concentration (IC_{50}) values show that the efficacy with which both **1** and **2** inhibit the prokaryotic ribosome is significantly lower than that of gentamicin and paromomycin. These data are in accordance with the observed antibacterial data of this set of compounds (Table 1). Thus, while both gentamicin and paromomycin exhibit excellent antibacterial activities against *Escherichia coli* (R477-100) with the minimal inhibitory concentrations (MIC) of 6 and 22 μM, respectively, both **2** and **1** lack significant antibacterial activity (MIC values of 588 and 790 μM, respectively). Similar correlation between prokaryotic antitranslational activity and MIC values in *E. coli* has previously been reported [39].

Discussion

A major concern that arises with the potential use of aminoglycosides for "translational therapy" is their toxicity to the organism preventing their repeated long-term administration required for the treatment of genetic diseases [7]. The results of this study show that compound **2**, the newly developed aminoglycoside, exhibits several folds greater suppression activity and far lower toxicity than those of gentamicin and paromomycin. This finding places compound **2** on the top among all the natural and/or synthetic aminoglycosides reported to date for the potential use in translational therapy.

The most compelling evidence for the superior readthrough efficiency of compound **2** over that of compound **1**, gentamicin and paromomycin was demonstrated *in vitro* on seven different DNA fragments derived from the mutant *PCDH15, CFTR, Dystrophin* and *IDUA* genes carrying nonsense mutations and representing the underlying causes for the genetic diseases USH1, CF, DMD and HS, respectively (Figure 2). Similar advantage of **2** was also demonstrated *ex vivo* in cultured cell lines (Figure 3). The presence of the flexible N-1-AHB group in compound **2** most likely contributes to its elevated readthrough efficiency compared to that of its parent compound **1**. This is consistent with previous reports showing that amikacin (N-1-AHB-kanamycin A) suppresses premature stop codons more efficiently than kanamycin A [5, 14]. Here we show that compound **2** binds the human cytoplasmic rRNA A-site sequence with a greater affinity than compound **1** (Figure 5), suggesting that the enhanced readthrough activity of **2** relative to **1** is due, at least in part, to a correspondingly enhanced affinity for the rRNA A-site. The impact of N-1-AHB group on the elevated readthrough activity of **2** was coupled with a lower toxicity profile of **2** (Table 1). Comparative acute lethal toxicity in mice, cell toxicity in three different kidney-derived cell lines and the assessment of hair cell toxicity in cochlear explants (Figure 4) clearly indicated that compound **2** is one of the least toxic aminoglycoside derivatives reported to date.

Even though many avenues of research have been pursued during the past few decades in an attempt to alleviate the aminoglycoside-induced toxicity to mammals [1, 7], few have been implemented into standard clinical use other than changes in administration schedule. Currently, only a limited number of aminoglycosides, including gentamicin, amikacin and tobramycin, are in clinical use as antibiotics for internal administration in humans. Among these, tobramycin does not have suppression activity, and gentamicin is the only one tested in clinical trials 10–12. Some recent studies in cultured cells and in animal models have shown that due to its relatively low toxicity, amikacin [14] may represent an alternative to gentamicin

for translational therapy. However, no clinical trials with amikacin have yet been reported, probably because of its significantly lower readthrough potency (over 10-fold lower) as compared to that of gentamicin [5, 14] (see Figure 2 and Figure S1 of Supporting Information). Furthermore, even though amikacin is less toxic than gentamicin and tobramycin [17], its acute intravenous toxicity in mice is significantly higher (LD_{50} = 300 mg/kg) [17] than that of compound **2** (LD_{50} = 500 mg/kg, Table 1).

In summary, the newly developed aminoglycoside compound **2** exhibits both appreciably higher suppression efficiency and lower toxicity than those of gentamicin. This achievement has several important implications. First, these results prove the principle that the mammalian ribosome can be effectively targeted by an aminoglycoside-based structure for improving suppression efficiency and reducing toxicity [7, 15, 22]. Second, the observed inability of **1** and **2** to show significant antibacterial activity along with their decreased prokaryotic ribosome specificity, are striking and remain to be further investigated. Of greatest concern is whether these data are linked or not to the observed reduced cell-and ototoxicity potential of **1** and **2**. This notion is supported by the fact that the mammalian mitochondrial protein synthesis machinery is very similar to the prokaryotic machinery [40] and that the aminoglycoside-induced ototoxicity may, at least in part, be connected to drug-mediated dysfunction of the mitochondrial ribosome [41, 42]. Third, the observed relatively low toxicity and high degree of potency of compound **2** in targeting all seven different nonsense constructs underlying USH1, CF, DMD and HS, support the feasibility of testing this novel aminoglycoside in treating these diseases in animal and human subjects. Finally, this study provides a new direction for the development of novel aminoglycoside-based structures by means of optimizing drug-induced suppression efficacy and toxicity; further progress in this direction may offer promise for the treatment of many genetic diseases caused by nonsense mutations.

Experimental Section

General

Paromomycin, amikacin, kanamycin A and gentamicin were purchased from Sigma. All other chemicals and biochemicals, unless otherwise stated, were obtained from commercial sources. In all biological tests, all the tested aminoglycosides were in their sulfate salt forms [Mw (gr/mol) of the sulfate salts were as follow: paromomycin – 713.7; gentamicin – 653.2; amikacin – 781.8; kanamycin A – 680.6; compound **1** – 563.0; compound **2** – 652.8]. Purity of the compounds **1** and **2** were determined by using HPLC-ESI-MS analysis which indicated 98.69% and 95.55% purity, respectively (see Supporting Information).

General methods

NMR spectra (including ^{1}H, ^{13}C, DEPT, 2D-COSY, 1D TOCSY, HMQC, HMBC) were routinely recorded on a Bruker Avance™ 500 spectrometer, and chemical shifts reported (in ppm) are relative to internal Me_4Si (δ =0.0) with $CDCl_3$ as the solvent, and to HOD (δ =4.63) with D_2O as the solvent. ^{13}C NMR spectra were recorded on a Bruker Avance™ 500 spectrometer at 125.8 MHz, and the chemical shifts reported (in ppm) relative to the residual solvent signal for $CDCl_3$ (δ =77.00), or to external sodium 2,2-dimethyl-2-silapentane sulfonate (δ =0.0) for D_2O as the solvent. Mass spectra analysis were obtained either on a Bruker Daltonix Apex 3 mass spectrometer under electron spray ionization (ESI), or by a TSQ-70B mass spectrometer (Finnigan Mat). Reactions were monitored by TLC on Silica Gel 60 F_{254} (0.25 mm, Merck), and spots were visualized by charring with a yellow solution containing $(NH_4)_6Mo_7O_{24}{\cdot}4H_2O$ (120 g) and $(NH_4)_2Ce(NO_3)_6$ (5 g) in 10% H_2SO_4 (800 mL). Flash column chromatography was performed on Silica Gel 60 (70–230 mesh). All reactions were carried out under an argon atmosphere with anhydrous solvents, unless otherwise noted.

2',3-Diazido-1-N-[(tert-butoxy)carbonyl]paromamine (4)—$Zn(OAc)_2$ (14.75 g, 66 mmol) was added to a stirred solution of paromamine (compound **3** in its free base form, 9.69 g, 30 mmol)) in H_2O (30 mL) and DMF (150 mL), and the mixture was stirred for 12 hours at room temperature. A solution of di-*tert*-butyldicarbonate (9.81 g, 45 mmol) in DMF (20 mL) was added to the reaction mixture over a time period of 30 minutes and the mixture was stirred for an additional 24 hours. The reaction progress was monitored by TLC [CH_2Cl_2/MeOH/H_2O/$MeNH_2$(33% solution in EtOH), 10:15:6:15]. The reaction mixture was diluted with MeOH (250 mL) and loaded onto 50×300 mm ion-exchange column (Amberlite CG50, H^+ form). The column was first washed extensively (about 10 column volumes) with a mixture MeOH/H_2O (60:40), followed by elution with the mixture of MeOH/H_2O/NH_4OH(25% solution in water) (80:15:5) to afford the desired N-1-Boc derivative of paromamine in 40% yield (5.03 g). ^{1}H NMR (500 MHz, D_2O): "Ring I": δ_H 2.70 (dd, 1H, J_1 = 3.5, J_2 = 7.0 Hz, H-2), 3.26 (dd, 1H, $J_1 = J_2$ = 9.5 Hz, H-4), 3.43 (dd, 1H, $J_1 = J_2$ = 9.5 Hz, H-3), 3.62 (dd, 1H, J_1 = 4.0, J_2 = 12.5 Hz, H-6'), 3.69 (dt, 1H, J_1 = 2.0, J_2 = 10.0 Hz, H-5), 3.72 (dd, 1H, J_1 = 4.0, J_2 = 12.5 Hz, H-6), 5.14 (d, 1H, J = 4.0 Hz, H-1); "Ring II": δ_H 1.18 (ddd, 1H, $J_1 = J_2 = J_3$ = 12.5 Hz, H-2ax), 2.51 (dt, 1H, J_1 = 4.5, J_2 = 12.5 Hz, H-2eq), 2.73-2.78 (m, 1H, H-3), 3.15 (dd, 1H, $J_1 = J_2$ = 9.5 Hz, H-4), 3.16 (dd, 1H, $J_1 = J_2$ = 10.0 Hz, H-6), 3.29-3.37 (m, 1H, H-1), 3.58 (dd, 1H, $J_1 = J_2$ = 10.0 Hz, H-5); the additional peaks in the spectrum were identified as follows: δ_H 1.30 (s, 9H, Boc). ^{13}C NMR (125 MHz, D_2O) "Ring I": δ_C 56.9 (C-2), 62.4 (C-6), 71.6 (C-4), 74.7 (C-5), 77.7 (C-3), 102.6 (C-1); "Ring II": δ_C 36.3 (C-2), 50.9 (C-3), 52.0 (C-1), 75.3 (C-5), 76.4 (C-6), 88.6 (C-4); the additional peaks in the spectrum were identified as follow: δ_C 29.4 (Boc, 3C), 159.6 (Boc, CO). MALDI TOFMS calculated for $C_{17}H_{33}N_3O_9Na$ ($[M+Na]^+$ *m/e* 446.2; measured *m/e* 446.5).

The product from the above step (44.3 g, 0.1 mol) was converted to the corresponding 3,2'-diazido derivative by following the published procedure [43], using Tf_2O (110 mL, 0.66 mol) and NaN_3 (100 g, 1.53 mol). The reaction progress was monitored by TLC (EtOAc/MeOH 95:5), which indicated completion after 8 hours. The crude product was purified by flash chromatography (EtOAc/MeOH 95:5) to yield the title compound **4** (42.5 g, 90% yield). ^{1}H NMR (500 MHz, MeOD): "Ring I": δ_H 2.88-2.93 (m, 1H, H-2), 3.23 (dd, 1H, $J_1 = J_2$ = 9.0 Hz, H-4), 3.49 (d, 2H, J_1 = 3.5 Hz, H-6, H-6'), 3.59-3.63 (m, 2H, H-3, H-5), 5.54 (d, 1H, J = 3.5 Hz, H-1); "Ring II": δ_H 1.08-1.16 (m, 1H, H-2ax), 1.96 (dt, 1H, J_1 = 4.0, J_2 = 12.5 Hz, H-2eq), 2.88-2.93 (m, 1H, H-6), 3.09-3.16 (m, 1H, H-1), 3.12-3.18 (m, 1H, H-3), 3.18 (dd, 1H, $J_1 = J_2$ = 9.5 Hz, H-4), 3.23 (dd, 1H, $J_1 = J_2$ = 9.0 Hz, H-5); the additional peaks in the spectrum were identified as follows: δ_H 1.13 (s, 9H, Boc). ^{13}C NMR (125 MHz, MeOD) "Ring I": δ_C 63.8 (C-6), 66.5 (C-2), 73.1 (C-4), 74.5 (C-3), 75.6 (C-5), 101.2 (C-1); "Ring II": δ_C 36.2 (C-2), 53.5 (C-1), 62.9 (C-3), 77.6 (C-6), 79.1 (C-5), 83.1 (C-4); the additional peaks in the spectrum were identified as follow: δ_C 31.1 (Boc, 3C), 160.0 (Boc, CO). MALDI TOFMS calculated for $C_{17}H_{29}N_7O_9$ K ($[M+K]^+$) *m/e* 514.2; measured *m/e* 514.4).

2',3-Diazido-1-N-[(S)-4-azido-2-hydroxy-butanoyl]paromamine (5)—Compound **4** (3.0 g, 6.31 mmol) was dissolved in a mixture of trifluoroacetic acid (12 mL) and dichloromethane (30 mL). The reaction progress was monitored by TLC (CH_2Cl_2/MeOH 4:1), which indicated completion after 1 hour. The reaction mixture was concentrated to dryness under reduced pressure. The resulting crude was dissolved in a mixture of Et_3N (10 mL) and DMF (10 mL) and cooled to −20°C. In a separate flask, (*S*)-2-hyroxy-4-azidobutyric acid (3.94 g, 31.55 mmol) was dissolved in anhydrous DMF (30 mL) and cooled to 0°C. To the cold solution, DCC (7.10 g, 34.46 mmol) and HOBT (4.72 g, 34.96 mmol) were added and the resulted mixture was stirred at 0°C for about one hour. This mixture was carefully added by syringe to the cold solution of the amine at −20°C. The reaction was stirred at −20°C for 1 hour and then allowed to warm to room temperature for an additional 1 hour. Thereafter, the mixture was treated with a solution of $MeNH_2$ (33 % solution in EtOH, 30 mL) and the reaction progress was monitored by TLC (CH_2Cl_2/MeOH 7:3). After completion of the reaction (about 8 hours)

the mixture was concentrated and purified by flash chromatography (MeOH/CH_2Cl_2 1:9) to provide the titled compound **5** (3.0 g, 93% yield). ^{1}H NMR (500 MHz, MeOD): "Ring I": δ_H 3.12 (dd, 1H, J_1 = 4.0, J_2 = 10.0 Hz, H-2), 3.45 (dd, 1H, J_1 = 9.5, J_2 = 10.5 Hz, H-4), 3.76-3.83 (m, 2H, H-6, H-6'), 3.92 (dd, 1H, J_1 = 9.0, J_2 = 10.5 Hz, H-3), 3.97-4.00 (m, 1H, H-5), 5.65 (d, 1H, J = 3.5 Hz, H-1); "Ring II": δ_H 1.55 (ddd, 1H, $J_1 = J_2 = J_3$ = 12.5 Hz, H-2ax), 2.18 (dt, 1H, J_1 = 4.0, J_2 = 13.0 Hz, H-2eq), 3.36 (dd, 1H, $J_1 = J_2$ = 9.0 Hz, H-6), 3.42-3.48 (m, 1H, H-3), 3.50 (dd, 1H, $J_1 = J_2$ = 9.0 Hz, H-4), 3.54 (dd, 1H, $J_1 = J_2$ = 9.0 Hz, H-5), 3.77-3.83 (m, 1H, H-1); the additional peaks in the spectrum were identified as follow: 1.82-1.88 (m, 1H, H-9), 2.01-2.07 (m, 1H, H-9), 3.46 (dd, 2H, J_1 = 6.5 J_2 =7.5, H-10), 4.16 (dd, 1H, J_1 = 4.0, J_2 = 8.5, H-8). ^{13}C NMR (125 MHz, MeOD) "Ring I": δ_C 61.0 (C-6), 63.6 (C-2), 70.6 (C-4), 71.3 (C-3), 72.8 (C-5), 98.3 (C-1); "Ring II": δ_C 32.3 (C-2), 49.1 (C-1), 60.2 (C-3), 74.6 (C-6), 77.4 (C-5), 79.7 (C-4); the additional peaks in the spectrum were identified as follow: 33.6 (C9), 47.4 (C10), 69.0 (C8), 175.7 (C7). MALDI TOFMS calculated for $C_{16}H_{26}N_{10}O_9$ K ([M +K]$^+$) *m/e* 541.2; measured *m/e* 541.1).

3',4',6',6-Tetra-O-acetyl-2',3-diazido-1-N-[(S)-4-azido-2-O-acetyl-butanoyl] paromamine (6)—Compound **5** (3.0 g, 5.85 mmol) was dissolved in dry pyridine (10 mL), cooled at −12°C and then acetic anhydride (5.4 equiv, 3.0 mL, 31.80 mmol) was added. The reaction temperature was kept at −12°C and the reaction progress was monitored by TLC (EtOAc/Hexane 7:3), which indicated completion after 8 hours. The reaction mixture was diluted with EtOAc (100 mL) and extracted with aqueous solution of HCl (2%), saturated aqueous $NaHCO_3$, and brine. The combined organic layer was dried over $MgSO_4$ and concentrated. The crude product was purified by flash chromatography (EtOAc/Hexane 2:3) to afford **6** (3.15 g, 75% yield). ^{1}H NMR (500 MHz, $CDCl_3$): "Ring I": δ_H 3.70 (dd, 1H, J_1 = 3.0, J_2 = 11.0 Hz, H-2), 4.10 (dd, 1H, J_1 = 2.0, J_2 = 12.5 Hz, H-6), 4.31 (dd, 1H, J_1 = 4.5, J_2 = 12.5 Hz, H-6'), 4.36-4.39 (m, 1H, H-5), 5.05 (dd, 1H, J_1 = 10.0, J_2 = 10.0 Hz, H-4), 5.28 (d, 1H, J = 3.5 Hz, H-1) 5.50 (dd, 1H, J_1 = 10.0, J_2 = 10.0 Hz, H-3); "Ring II": δ_H 1.48 (ddd, 1H, $J_1 = J_2 = J_3$ = 12.5 Hz, H-2ax), 2.50 (dt, 1H, J_1 = 4.0, J_2 = 13.0 Hz, H-2eq), 3.34-3.39 (m, 1H, H-4), 3.38-3.43 (m, 1H, H-3), 3.74-3.78 (m, 1H, H-5), 3.99-4.04 (m, 1H, H-1), 4.82 (dd, 1H, $J_1 = J_2$ = 10.0 Hz, H-6), 6.63 (d, 1H, J = 7.5 Hz, NH); the additional peaks in the spectrum were identified as follow: 2.05-2.09 (m, 2H, H-9), 2.05 (s, 3H, Ac), 2.08 (s, 3H, Ac), 2.09 (s, 3H, Ac), 2.15 (s, 3H, Ac), 2.19 (s, 3H, Ac), 3.35-3.38 (m, 2H, H-10), 5.14 (dd, 1H, J_1 = 5.5, J_2 = 6.5, H-8). ^{13}C NMR (125 MHz, $CDCl_3$) "Ring I": δ_C 61.8 (C-6), 61.8 (C-2), 68.1 (C-4), 68.4 (C-5), 71.4 (C-3), 99.1 (C-1); "Ring II": δ_C 32.5 (C-2), 48.2 (C-1), 58.2 (C-3), 73.8 (C-5), 74.0 (C-6), 84.3 (C-4); the additional peaks in the spectrum were identified as follow: 20.6-20.9 (Ac, 5C), 30.5 (C-9), 47.1 (C-10), 70.8 (C8), 169.1 (C-8, CO), 169.8 (Ac, CO), 169.8 (C-7, CO), 170.0 (Ac, CO), 170.6 (Ac, CO), 172.4 (Ac, CO). MALDI TOFMS calculated for $C_{26}H_{36}N_{10}O_{14}$ K ([M+K]$^+$) *m/e* 751.2; measured *m/e* 751.1).

5-O-(5-Azido-2,3-O-dibenzoyl-5-deoxy-β-D-ribofuranosyl)-3',4',6',6-tetra-O-acetyl-2',3-diazido-1-N-[(S)-4-azido-2-O-acetyl-butanoyl]paromamine (8)— Anhydrous CH_2Cl_2 (10 mL) was added to a powdered, flame-dried 4 Å molecular sieves (3.0 g), followed by the addition of the acceptor (compound **6**, 1.75 g, 2.46 mmol) and the donor (compound 7, 5-deoxy-5-azido-2,3-di-*O*-benzoyl-1-*O*-trichloroacetimido-D-ribofuranose) [15] (3.3 g, 6.27 mmol) dissolved in CH_3CN (10 mL). The mixture was stirred for 10 min at room temperature and was then cooled to −20°C. A catalytic amount of BF_3-Et_2O (100 μl) was added and the mixture was stirred at −15 °C. The reaction progress was monitored by TLC (EtOAc/Hexane 3:2), which indicated the completion after 30 min. The reaction was diluted with CH_2Cl_2 and filtered through celite. After thorough washing of the celite with CH_2Cl_2, the washes were combined and extracted with saturated aqueous $NaHCO_3$, brine, dried over $MgSO_4$ and concentrated. The crude product was purified by flash chromatography (EtOAc/Hexane 2:3) to afford compound **8** (2.01 g, 76% yield). ^{1}H NMR (500 MHz, $CDCl_3$): "Ring

I": δ_H 3.53 (dd, 1H, J_1 = 4.0, J_2 = 11.0 Hz, H-2), 4.15 (dd, 1H, J_1 = 2.0, J_2 = 12.5 Hz, H-6), 4.26 (dd, 1H, J_1 = 4.0, J_2 = 12.5 Hz, H-6'), 4.50-4.55 (m, 1H, H-5), 5.07 (dd, 1H, J_1 = 9.5, J_2 = 10.0 Hz, H-4), 5.43 (dd, 1H, J_1 = 9.5, J_2 = 10.0 Hz, H-3), 5.83 (d, 1H, J = 4.0 Hz, H-1); "Ring II": δ_H 1.47 (ddd, 1H, J_1 = J_2 = J_3 = 12.5 Hz, H-2ax), 2.50 (dt, 1H, J_1 = 4.0, J_2 = 13.0 Hz, H-2eq), 3.56-3.58 (m, 1H, H-3), 3.72 (dd, 1H, J_1 = 8.5, J_2 = 9.5 Hz, H-4), 3.99 (dd, 1H, J_1 = 8.5, J_2 = 9.5 Hz, H-5), 4.01-4.08 (m, 1H, H-1), 4.91 (dd, 1H, J_1 = 9.5, J_2 = 10.5 Hz, H-6), 6.64 (d, 1H, J = 8.5 Hz, NH); "Ring III": δ_H 3.57 (dd, 1H, J_1 = 6.0, J_2 = 13.0 Hz, H-5'), 3.64 (dd, 1H, J_1 = 3.0, J_2 = 13.0 Hz, H-5), 4.50-4.55 (m, 1H, H-4), 5.49 (dd, 1H, J_1 = 5.0, J_2 = 7.0 Hz, H-3), 5.62 (dd, 1H, J_1 = 1.0, J_2 = 5.0 Hz, H-2), 5.68 (d, 1H, J = 1.0 Hz, H-1); the additional peaks in the spectrum were identified as follow: 2.00-2.15 (m, 2H, H-9), 2.04 (s, 3H, Ac), 2.09 (s, 6H, 2Ac), 2.20 (s, 3H, Ac), 2.23 (s, 3H, Ac), 3.35 (t, 2H, J = 7.0, H-10), 5.16 (dd, 1H, J_1 = 5.0, J_2 = 7.0, H-8), 7.33 (t, 2H, J = 8.0, Bz), 7.43 (t, 2H, J = 8.0, Bz), 7.51-7.54 (m, 1H, Bz), 7.56-7.60 (m, 1H, Bz), 7.85 (dd, 2H, J = 1.0, 7.5, Bz), 7.94 (dd, 2H, J = 1.0, 7.5, Bz). ^{13}C NMR (125 MHz, $CDCl_3$) "Ring I": δ_C 61.6 (C-2), 61.8 (C-6), 68.1 (C-5), 68.2 (C-4), 70.7 (C-3), 96.8 (C-1); "Ring II": δ_C 32.1 (C-2), 48.4 (C-1), 58.5 (C-3), 73.5 (C-6), 77.9 (C-4), 80.0 (C-5); "Ring III": δ_C 52.7 (C-2), 71.5 (C-3), 74.7 (C-2), 80.1 (C-4), 107.4 (C-1); the additional peaks in the spectrum were identified as follow: 20.6-20.9 (Ac, 5C), 30.5 (C-9), 47.1 (C-10), 70.9 (C8), 128.4 (Bz, 2C), 128.5 (Bz, 2C), 129.6 (Bz, 2C), 129.7 (Bz, 2C), 133.6 (Bz, 1C), 133.7 (Bz, 1C), 165.2 (Bz, CO), 165.2 (Bz, CO), 168.9 (C-8, CO), 169.7 (Ac, CO), 169.7 (C-7, CO), 169.9 (Ac, CO), 170.6 (Ac, CO), 172.3 (Ac, CO). MALDI TOFMS calculated for $C_{45}H_{51}N_{13}O_{19}$ K ($[M+K]^+$) *m/e* 1116.3; measured *m/e* 1116.3.

5-O-(5-Amino-5-deoxy-β-D-ribofuranosyl)-1-N-[(S)-4-amino-2-hydroxy-butanoyl]paromamine (2)—Compound **8** (1.55 g, 1.44 mmol) was treated with a solution of $MeNH_2$ (33% solution in EtOH, 50 mL) and the reaction progress was monitored by TLC (EtOAc/MeOH 85:15), which indicated completion after 8 hours. The reaction mixture was evaporated to dryness and the residue was dissolved in a mixture of THF (5 mL) and aqueous NaOH (1 mM, 5.0 mL). The mixture was stirred at room temperature for 10 minutes, after which PMe_3 (1 M solution in THF, 11.52 mL, 11.52 mmol) was added. The reaction progress was monitored by TLC [CH_2Cl_2/MeOH/H_2O/$MeNH_2$ (33% solution in EtOH) 10:15:6:15], which indicated completion after 1 hour. The product was purified by flash chromatography on a short column of silica gel. The column was washed with the following solvents: THF (800 mL), CH_2Cl_2 (800 mL), EtOH (200 mL), and MeOH (400 mL). The product was then eluted with a mixture of 20% $MeNH_2$ (33% solution in EtOH) in 80% MeOH. Fractions containing the product were combined and evaporated to dryness. The residue was re-dissolved in a small volume of water and evaporated again (2–3 repeats) to afford the free amine form of **2**. The analytically pure product was obtained by passing the above product through a short column of Amberlite CG50 (NH_4^+ form). The column was first washed with a mixture of MeOH/H_2O (3:2), then the product was eluted with a mixture of MeOH/H_2O/NH_4OH (80:10:10) to afford compound **2** (628 mg, 78% yield).

For the storage and biological tests, **2** was converted to its sulfate salt form: the free base was dissolved in water, the pH was adjusted to 6.5 with H_2SO_4 (0.1 N) and lyophilized. ^{1}H NMR (500 MHz, D_2O, pD 3.5) "Ring I": δ_H 3.52 (dd, 1H, J_1 = 4.0, J_2 = 11.0 Hz, H-2), 3.53-3.57 (m, 1H, H-4), 3.81-3.85 (m, 1H, H-5), 3.81-3.85 (m, 1H, H-6), 3.93-3.98 (m, 1H, H-6'), 4.04 (dd, 1H, J_1 = 9.0, J_2 = 10.0 Hz, H-3), 5.87 (d, 1H, J = 4.0 Hz, H-1); "Ring II": δ_H 1.80 (ddd, 1H, J_1 = J_2 = J_3 = 12.5 Hz, H-2ax), 2.24 (dt, 1H, J_1 = 4.0, J_2 = 12.5 Hz, H-2eq), 3.54-3.58 (m, 1H, H-3), 3.73 (dd, 1H, J_1 = J_2 = 9.5 Hz, H-6), 3.92-3.98 (m, 1H, H-1), 3.99 (dd, 1H, J_1 = J_2 = 9.0 Hz, H-5), 4.11 (dd, 1H, J_1 = J_2 = 9.5 Hz, H-4); "Ring III": δ_H 3.29 (dd, 1H, J_1 = 7.0, J_2 = 13.5 Hz, H-5), 3.42 (dd, 1H, J_1 = 4.0, J_2 = 13.5 Hz, H-5'), 4.12-4.15 (m, 1H, H-4), 4.23-4.25 (m, 1H, H-3), 4.26-4.29 (m, 1H, H-2), 5.40 (s, 1H, H-1); the additional peaks in the spectrum were identified as follow: 1.98-2.06 (m, 1H, H-9), 2.15-2.22 (m, 1H, H-9), 3.14-3.23 (m, 2H, H-10), 4.34 (dd, 1H, J_1= 4.0, J_2 = 8.5, H-8). ^{13}C NMR (125 MHz, D_2O) "Ring I": δ_C 55.4

(C-2), 61.9 (C-6), 70.8 (C-3), 70.8 (C-4), 75.8 (C-5), 95.7 (C-1); "Ring II": δ_C 31.4 (C-2), 50.4 (C-3), 51.4 (C-1), 74.6 (C-6), 78.1 (C-4), 85.1 (C-5); "Ring III": δ_C 43.4 (C-5), 72.7 (C-3), 76.5 (C-3), 79.9 (C-4), 110.5 (C-1); the additional peaks in the spectrum were identified as follow: 32.6 (C9), 38.4 (C10), 71.3 (C8), 177.4 (C7). MALDI TOFMS calculated for $C_{21}H_{41}N_5O_{12}$ K ($[M+K]^+$) *m/e* 594.3; measured *m/e* 594.3.

Dual luciferase readthrough assays

DNA fragments derived from PCDH15, CFTR, Dystrophin and IDUA cDNAs, including the tested nonsense mutation or the corresponding wt codon, and four to six upstream and downstream flanking codons were created by annealing following pairs of complementary oligonucleotides. *p.R3Xmut/wt*: 5'-GATCCCAGAAGATGTTTT/ CGACAGTTTTATCTCTGGACAGAGCT-3' and 5'-CTGTCAGAGATAAAACTGTCA/ GAAACATCTTCTG-3'; *p.R245Xmut/wt*: 5'-GATCCAAAATCTGAATGAGAGGT/ CGAACCACCACCACCACCCTCGAGCT-3' and 5'-CGAGGGTGGTGGTGGTTGTTCG/ ACCTCTCATTCAGATTTTG-3'; *p.G542Xmut/wt*: 5'-TCGACCAATATAGTTCTTT/ GGAGAAGGTGGAATCGAGCT-3' and 5'-CGATTCCACCTTCTCA/ GAAGAACTATATTGG-3'; *p.W1282Xmut/wt*: 5'-TCGACAACTTTGCAACAGTGA/ GAGGAAAGCCTTTGAGCT-3' and 5'-CAAAGGCTTTCCTT/ CCACTGTTGCAAAGTTG-3'; *p.R3381Xmut/wt*: 5'-TCGACAAAAAACAAATTTTGA/ CACCAAAAGGTATGAGCT-3' and 5'-CATACCTTTTGGTT/ GCAAAATTTGTTTTTTG-3'; *p.Q70Xmut/wt*: 5'-TCGACCCTCAGCTGGGACT/ CAGCAGCTCAACCTCGAGCT-3' and 5'-CGAGGTTGAGCTGCTA/ GGTCCCAGCTGAGG-3'; *p.W402Xmut/wt*: 5'-TCGACTGAGGAGCAGCTCTGA/ GGCCGAAGTGTCGGAGCT-3' and 5'-CCGACACTTCGGCT/ CCAGAGCTGCTCCTCAG-3'.

Fragments were inserted in frame into the polylinker of the p2Luc plasmid between either *BamHI* and *SacI* (*p.R3X and p.R245X*) or *SalI* and *SacI* (all the rest) restriction sites. For the *in vitro* readthrough assays, the obtained plasmids, with addition of the tested aminoglycosides were transcribed and translated using the TNT Reticulocyte Lysate Quick Coupled Transcription/Translation System. Luciferase activity was determined after 90 min of incubation at 30°C, using the Dual Luciferase Reporter Assay System. For the *ex vivo* readthrough assays the construct harboring the R3X mutation was transfected to COS-7 cells with Lipofectamine 2000 (Invitrogen) and addition of the tested compounds was performed 5 hours post transfection. Stop codon readthrough was calculated as previously described [27].

Toxicity assays

Cytotoxicity of compound **2** was determined as previously reported by us for gentamicin, paromomycin and compound **1** [16]. Male BALB/C mice at 22 days of age (18-20 g) purchased from Harlan Laboratories Limited (Jerusalem, Israel) were used to evaluate the LD_{50} of the aminoglycosides. Mice were maintained on a 12 h light/dark cycle at 20-22 °C, with relative humidity of 50-55%, and were given food and water ad libitum. The aminoglycosides tested were administered in single intravenous (i.v.) doses and each concentration was applied to 8 animals. The aminoglycosides were dissolved in PBS, and 150 μL of final solution (pH=7) were injected into the tail vein. Changes in the appearance and behavior, and mortality in mice were monitored for 4 days after the administration. The LD_{50} values were determined according to the Reed and Muench method [44].

For evaluation of ototoxicity, a preparation of the organ of Corti and spiral ganglion neurons was obtained by dissection of the cochlea from postnatal day 3 mice. The tissue was positioned as a flat surface preparation on a collagen-coated incubation dish in 1 mL of serum-free BME plus serum-free supplement (Sigma), 1% bovine serum albumin, 2 mM glutamine, 5 mg/mL

glucose and 10 U/mL penicillin and incubated for 4–5 h (37°C, 5% CO_2). Then an additional 1 mL of the culture medium was added and incubation continued for 24 h. The next day, the serum-free medium was exchanged for a new medium containing a specific concentration of drug and incubated for desired time points. For hair cell counts, organ cultures were fixed overnight in 4% paraformaldehyde at 4°C and then permeabilized for 30 min with 3% Triton X-100 in PBS. The specimens were washed three times with PBS and blocked with 10% goat serum for 30 min at room temperature, followed by incubation at room temperature for 40 min for fluorescent visualization of F-actin with rhodamine-phalloidin or Alexa 488-phalloidin (Molecular Probes). After several rinses in PBS, the specimens were mounted on a slide with fluoromount-G (SouthernBiotech).

UV Melting Studies

The human cytoplasmic rRNA A-site model oligonucleotide 5′-GGCGUCGCUACUUCGGUAAAAGUCGCC-3′ was obtained in its PAGE-purified sodium salt form from Dharmacon, Inc. (Chicago, IL). The concentrations of all RNA solutions were determined spectrophotometrically as previously described [36]. All experimental RNA solutions were preheated at 85 °C for 5 min and slowly cooled to room temperature prior to their use. Temperature-dependent absorption experiments were conducted on an AVIV Model 14DS spectrophotometer (Aviv Biomedical; Lakewood, NJ) equipped with a thermoelectrically controlled cell holder. Quartz cells with a 1 cm pathlength were used for all of the absorbance studies. Temperature-dependent absorption profiles (Fig. 5) were acquired at 274 nm with a 5 s averaging time. The temperature was raised in 0.5 °C increments, and the samples were allowed to equilibrate for 1.5 min at each temperature setting. In these UV melting studies, the RNA solutions were 2 μM in strand and drug concentrations ranged from 0 to 10 μM. Buffer solutions contained 10 mM EPPS (pH 7.0) and 10 mM NaCl.

Supplementary Material

Refer to Web version on PubMed Central for supplementary material.

Abbreviations

CF	cystic fibrosis
DMD	Duchenne muscular dystrophy
USH	Usher syndrome
HS	Hurler syndrome
CFTR	cystic fibrosis transmembrane conductance regulator
PCDH15	Protocadherin 15
USH1	Usher syndrome
AHB	(*S*)-4-amino-2-hydroxybutanoyl
Boc_2O	Di-tert-butyl dicarbonate
TFA	trifluoroacetic acid
HOBT	Hydroxybenzotriazole
DCC	N,N'-dicyclohexylcarbodiimide
BtrH	butirosin 1-*N*-acyltransferase
BtrG	butirosin 1-*N*-γ-L-glutamyl cyclotransferase

HEK-293	human embryonic kidney cell line
COS-7	monkey kidney cell line
MDCK	canine kidney cell line
LC_{50}	half-maximal lethal concentration
LD_{50}	half-maximal lethal dose
OHC	outer hair cells
IHC	inner hair cells
T_m	melting temperatures
MIC	minimal inhibitory concentrations
PBS	Phosphate buffered saline
EPPS	4-(2-Hydroxyethyl)-1-piperazinepropanesulfonic acid

Acknowledgments

The authors thank John F. Atkins (University of Utah) for providing the p2luc plasmid and Mrs. Larisa Panz for the purity determination of compounds **1** and **2**. This work supported by research grants from the US-Israel Binational Science Foundation (grant no. 2006/301) to T.B. and D.S.P., Horowitz Fund (grant no. 2010826) to T.B. and T.B.Y., RO1 DC03685 and P30 05188 from the National Institutes of Health to J.S., and the Foundation du Judaisme Francais to ARS. V.B. acknowledges the financial Support by the Center of Absorption in Science, the Ministry of Immigration Absorption and the Ministry of Science and Technology, Israel (Kamea Program).

REFERENCES

1. Keeling KM, Bedwell DM. Pharmacological suppression of premature stop mutations that cause genetic diseases. Curr. Pharmacogenomics 2005;3:259–269.
2. Mort M, Ivanov D, Cooper DN, Chuzhanova NA. A meta-analysis of nonsense mutations causing human genetic disease. Human Mutation 2008;29:1037–1047. [PubMed: 18454449]
3. Burke JF, Mogg AE. Suppression of a nonsense mutation in mammalian cells in vivo by the aminoglycoside antibiotics G-418 and paromomycin. Nucleic Acids Res 1985;13:6265–6272. [PubMed: 2995924]
4. Kaufman RJ. Correction of genetic disease by making sense from nonsense. J. Clin. Invest 1999;104:367–368. [PubMed: 10449426]
5. Manuvakhova M, Keeling K, Bedwell DM. Aminoglycoside antibiotics mediate context-dependent suppression of termination codons in a mammalian translation system. RNA 2000;6:1044–1055. [PubMed: 10917599]
6. Kerem E. Pharmacologic therapy for stop mutations: how much CFTR activity is enough? Curr. Opin. Pulm. Med 2004;10:547–552. [PubMed: 15510065]
7. Hainrichson M, Nudelman I, Baasov T. Designer aminoglycosides: the race to develop improved antibiotics and compounds for the treatment of human genetic diseases. Org. Biomol. Chem 2008;6:227–239. [PubMed: 18174989]
8. Barton-Davis ER, Cordier L, Shoturma DI, Leland SE, Sweeney HL. Aminoglycoside antibiotics restore dystrophin function to skeletal muscles of mdx mice. J. Clin. Invest 1999;104:375–381. [PubMed: 10449429]
9. Du M, Jones JR, Lanier J, Keeling KM, Lindsey JR, Tousson A, Bebok Z, Whitsett JA, Dey CR, Colledge WH, Evans MJ, Sorscher EJ, Bedwell DM. Aminoglycoside suppression of a premature stop mutation in a Cftr−/− mouse carrying a human CFTR-G542X transgene. J. Mol. Med 2002;80:595–604. [PubMed: 12226741]

10. Wilschanski M, Yahav Y, Yaacov Y, Blau H, Bentur L, Rivlin J, Aviram M, Bdolah-Abram T, Bebok Z, Shushi L, Kerem B, Kerem E. Gentamicin-induced correction of CFTR function in patients with cystic fibrosis and CFTR stop mutations. N. Engl. J. Med 2003;349:1433–1441. [PubMed: 14534336]
11. Politano L, Nigro G, Nigro V, Piluso G, Papparella S, Paciello O, Comi LI. Gentamicin administration in Duchenne patients with premature stop codon Preliminary results. Acta Myol 2003;22:15–21. [PubMed: 12966700]
12. Wagner KR, Hamed S, Hadley DW, Gropman AL, Burstein AH, Escolar DM, Hoffman EP, Fischbeck KH. Gentamicin treatment of Duchenne and Becker muscular dystrophy due to nonsense mutations. Ann. Neurol 2001;49:706–711. [PubMed: 11409421]
13. Ramalho AS, Beck S, Meyer M, Penque D, Cutting GR, Amaral MD. Five percent of normal cystic fibrosis transmembrane conductance regulator mRNA ameliorates the severity of pulmonary disease in cystic fibrosis. Am. J. Respir. Cell Mol. Biol 2002;27:619–627. [PubMed: 12397022]
14. Du M, Keeling KM, Fan L, Liu X, Kovacs T, Sorscher E, Bedwell DM. Clinical doses of amikacin provide more effective suppression of the human CFTR-G542X stop mutation than gentamicin in a transgenic CF mouse model. J. Mol. Med 2006;84:573–582. [PubMed: 16541275]
15. Nudelman I, Rebibo-Sabbah A, Shallom-Shezifi D, Hainrichson M, Stahl I, Ben-Yosef T, Baasov T. Redesign of aminoglycosides for treatment of human genetic diseases caused by premature stop mutations. Bioorg. Med. Chem. Lett 2006;16:6310–6315. [PubMed: 16997553]
16. Rebibo-Sabbah A, Nudelman I, Ahmed ZM, Baasov T, Ben-Yosef T. In vitro and ex vivo suppression by aminoglycosides of PCDH15 nonsense mutations underlying type 1 Usher syndrome. Hum. Genet 2007;122:373–381. [PubMed: 17653769]
17. Fujisawa K, Hoshiya T, Kawaguchi H. Aminoglycoside antibiotics. VII. Acute toxicity of aminoglycoside antibiotics. J. Antibiot. (Tokyo) 1974;27:677–681. [PubMed: 4436153]
18. Kondo S, Hotta K. Semisynthetic aminoglycoside antibiotics: Development and enzymatic modifications. J. Infect. Chemother 1999;5:1–9. [PubMed: 11810483]
19. Reiffens J, Holmes SW, Hottendo G, Bierwage M. Ototoxicity Studies with Bb-K8 - New Semisynthetic Aminoglycoside Antibiotic. J. Antibiot 1973;26:94–100. [PubMed: 4544451]
20. Kondo J, Francois B, Russell RJ, Murray JB, Westhof E. Crystal structure of the bacterial ribosomal decoding site complexed with amikacin containing the gamma-amino-alpha-hydroxybutyryl (haba) group. Biochimie 2006;88:1027–1031. [PubMed: 16806634]
21. Russell RJ, Murray JB, Lentzen G, Haddad J, Mobashery S. The complex of a designer antibiotic with a model aminoacyl site of the 30S ribosomal subunit revealed by X-ray crystallography. J. Am. Chem. Soc 2003;125:3410–3411. [PubMed: 12643685]
22. Kondo J, Hainrichson M, Nudelman I, Shallom-Shezifi D, Barbieri CM, Pilch DS, Westhof E, Baasov T. Differential Selectivity of Natural and Synthetic Aminoglycosides towards the Eukaryotic and Prokaryotic Decoding A Sites. ChemBioChem 2007;8:1700–1709. [PubMed: 17705310]
23. Kirst HA, Truedell BA, Toth JE. Control of Site-Specific Substitution of Aminoglycosides by Transition-Metal Cations. Tet. Lett 1981;22:295–298.
24. Fridman M, Belakhov V, Lee LV, Liang FS, Wong CH, Baasov T. Dual effect of synthetic aminoglycosides: antibacterial activity against Bacillus anthracis and inhibition of anthrax lethal factor. Angew. Chem. Int. Ed. Engl 2005;44:447–452. [PubMed: 15624157]
25. Nudelman I, Chen L, Llewellyn NM, Sahraoui EH, Cherniavsky M, Spencer JB, Baasov T. Combined chemical-enzymatic assembly of aminoglycoside derivatives with N-1-AHB side chain. Adv. Synth. Catal 2008;350:1682–1688.
26. Howard MT, Shirts BH, Petros LM, Flanigan KM, Gesteland RF, Atkins JF. Sequence specificity of aminoglycoside-induced stop condon readthrough: potential implications for treatment of Duchenne muscular dystrophy. Ann. Neurol 2000;48:164–169. [PubMed: 10939566]
27. Grentzmann G, Ingram JA, Kelly PJ, Gesteland RF, Atkins JF. A dual-luciferase reporter system for studying recoding signals. RNA 1998;4:479–486. [PubMed: 9630253]
28. Albiero L, Bamonte F, Ongini E, Parravicini L. Comparison of neuromuscular effects and acute toxicity of some aminoglycoside antibiotics. Arch. Int. Pharmacodyn. Ther 1978;233:343–350. [PubMed: 686918]

29. Rothlin CV, Katz E, Verbitsky M, Vetter DE, Heinemann SF, Elgoyhen AB. Block of the alpha9 nicotinic receptor by ototoxic aminoglycosides. Neuropharmacology 2000;39:2525–2532. [PubMed: 11044724]
30. Talbot PA. Potentiation of aminoglycoside-induced neuromuscular blockade by protons in vitro and in vivo. J. Pharmacol. Exp. Ther 1987;241:686–694. [PubMed: 3033223]
31. Paradelis AG, Triantaphyllidis C, Markomichelakis JM, Logaras G. The neuromuscular blocking activity of aminodeoxykanamycin as compared with that of other aminoglycoside antibiotics. Arzneimittel-Forschung 1977;27:141–143. [PubMed: 576814]
32. Amici M, Eusebi F, Miledi R. Effects of the antibiotic gentamicin on nicotinic acetylcholine receptors. Neuropharmacology 2005;49:627–637. [PubMed: 15936782]
33. Vital Brazil O, Prado-Franceschi J. The neuromuscular blocking action of gentamicin. Arch. Int. Pharmacodyn. Ther 1969;179:65–77. [PubMed: 4311767]
34. Sha SH, Qiu JH, Schacht J. Aspirin to prevent gentamicin-induced hearing loss. N. Engl. J. Med 2006;354:1856–1857. [PubMed: 16641409]
35. Forge A, Schacht J. Aminoglycoside antibiotics. Audiol. Neurootol 2000;5:3–22. [PubMed: 10686428]
36. Kaul M, Barbieri CM, Pilch DS. Defining the basis for the specificity of aminoglycoside-rRNA recognition: a comparative study of drug binding to the A sites of Escherichia coli and human rRNA. J. Mol. Biol 2005;346:119–134. [PubMed: 15663932]
37. Crothers DM. Statistical Thermodynamics of Nucleic Acid Melting Transitions with Coupled Binding Equilibria. Biopolymers 1971;10:2147–2160. [PubMed: 5118648]
38. Marky LA, Breslauer KJ. Calculating Thermodynamic Data for Transitions of Any Molecularity from Equilibrium Melting Curves. Biopolymers 1987;26:1601–1620. [PubMed: 3663875]
39. Greenberg WA, Priestley ES, Sears PS, Alper PB, Rosenbohm C, Hendrix M, Hung SC, Wong CH. Design and synthesis of new aminoglycoside antibiotics containing neamine as an optimal core structure: correlation of antibiotic activity with in vitro inhibition of translation. J. Am. Chem. Soc 1999;121:6527–6541.
40. Kondo J, Westhof E. The bacterial and mitochondrial ribosomal A-site molecular switches possess different conformational substates. Nucleic Acids Res 2008;36:2654–2666. [PubMed: 18346970]
41. Bottger EC, Springer B, Prammananan T, Kidan Y, Sander P. Structural basis for selectivity and toxicity of ribosomal antibiotics. EMBO Rep 2001;2:318–323. [PubMed: 11306553]
42. Hobbie SN, Bruell CM, Akshay S, Kalapala SK, Shcherbakov D, Bottger EC. Mitochondrial deafness alleles confer misreading of the genetic code. Proc. Natl. Acad. Sci. U. S. A 2008;105:3244–3249. [PubMed: 18308926]
43. Alper PB, Hendrix M, Sears PS, Wong CH. Probing the specificity of aminoglycoside-ribosomal RNA interactions with designed synthetic analogs. J. Am. Chem. Soc 1998;120:1965–1978.
44. Reed LJ, Muench H. A simple method for estimating fifty per cent endpoints. Am. J. Hyg 1938;27:493–496.

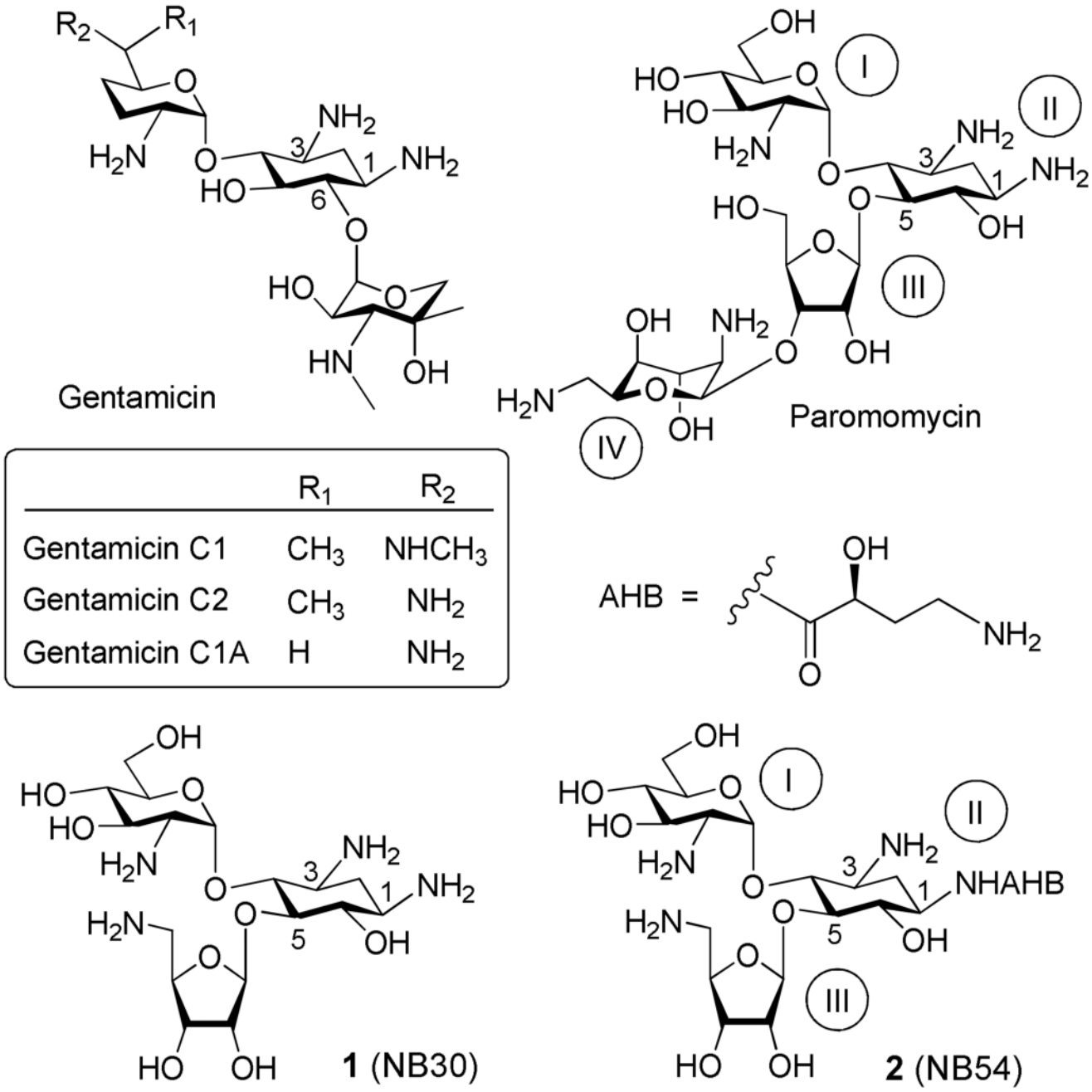

	R_1	R_2
Gentamicin C1	CH_3	$NHCH_3$
Gentamicin C2	CH_3	NH_2
Gentamicin C1A	H	NH_2

Figure 1.
Chemical structures of a series of 2-deoxystreptamine-derived (ring II) aminoglycosides, including gentamicin, paromomycin, **1** and **2** that were investigated in this study.

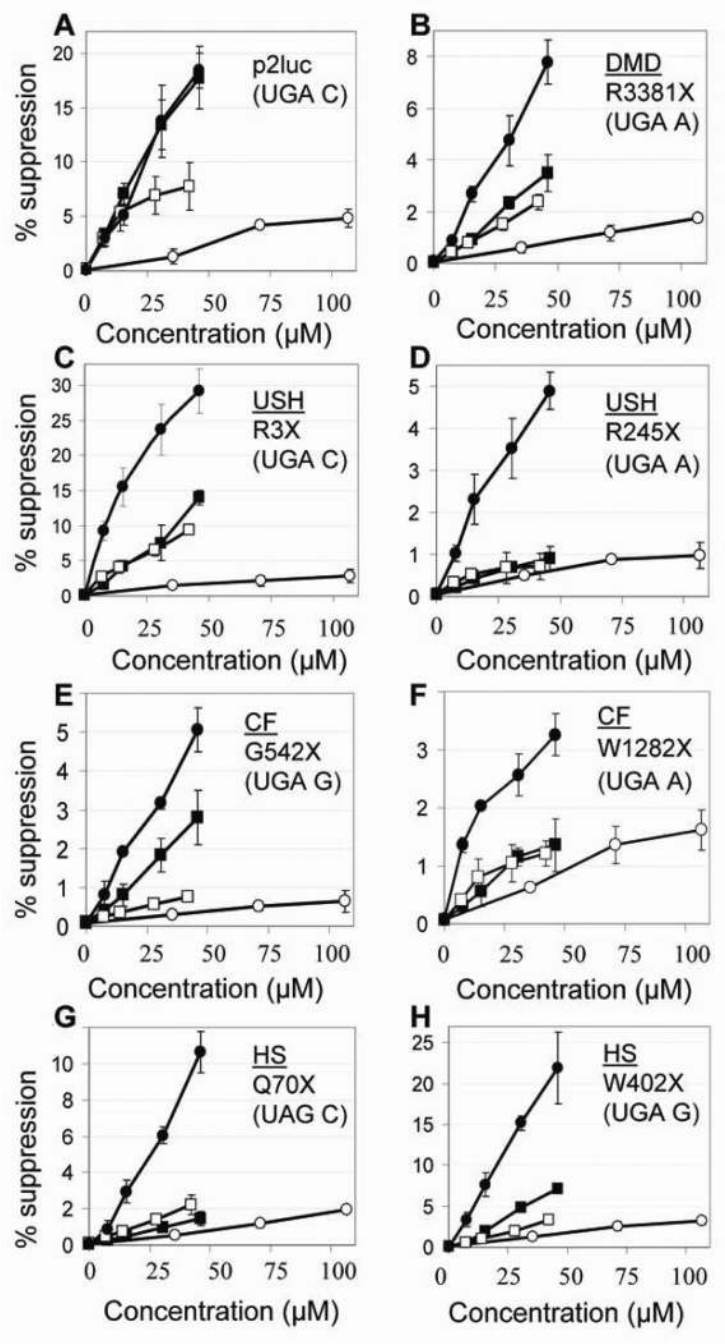

Figure 2.

In-vitro stop codon suppression levels induced by compound **2** (●), gentamicin (■), paromomycin (□) and compound **1** (○) in a series of nonsense mutation context constructs representing various genetic diseases (shown in parenthesis): (A) p2luc, (B) R3381X (DMD), (C) R3X (USH1), (D) R245X (USH1), (E) G542X (CF), (F) W1282X (CF), (G) Q70X (HS), (H) W402X (HS). DNA fragments were cloned between BamHI and SacI restriction sites of the p2luc vector and the obtained constructs were transcribed and translated using TNT quick coupled transcription/translation system. The amount of the translated products was evaluated using the dual luciferase reporter assay system and the suppression level was calculated as described previously [27]. The results are averages of at least three independent experiments.

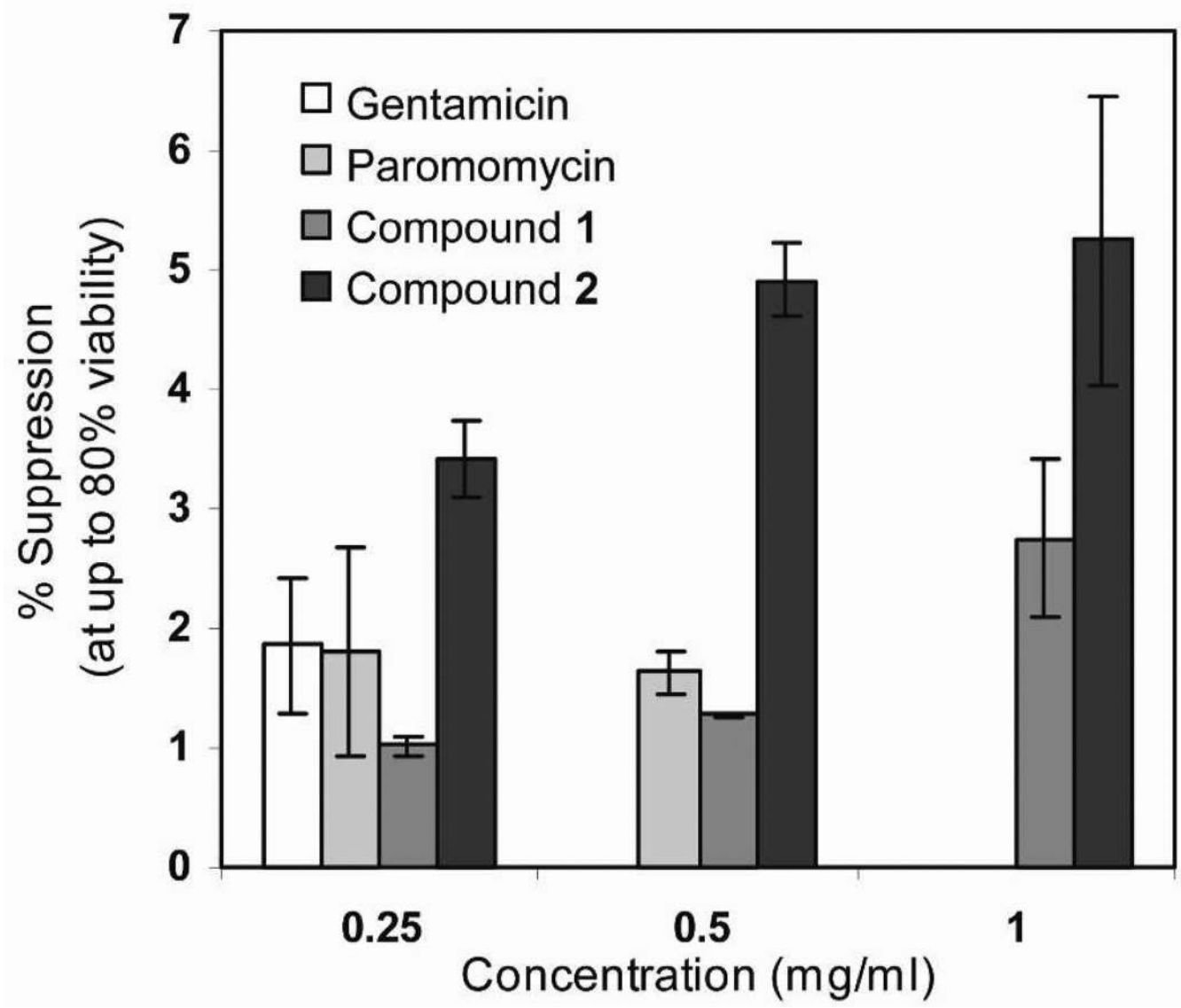

Figure 3.

Ex vivo suppression of the *PCDH15*-R3X nonsense mutation by **1**, **2**, paromomycin and gentamicin. The p2Luc plasmid harboring the R3X nonsense mutation (containing four upstream and six downstream *PCDH15*-flanking codons) inserted in frame between the renilla luciferase and firefly luciferase genes was transfected into COS-7 cells and addition of tested compounds was performed after 5 hours. Luciferase activity was determined using the Dual Luciferase Reporter Assay System (Promega). Stop codon readthrough was calculated as described previously [27]. The results are averages of at least three independent experiments.

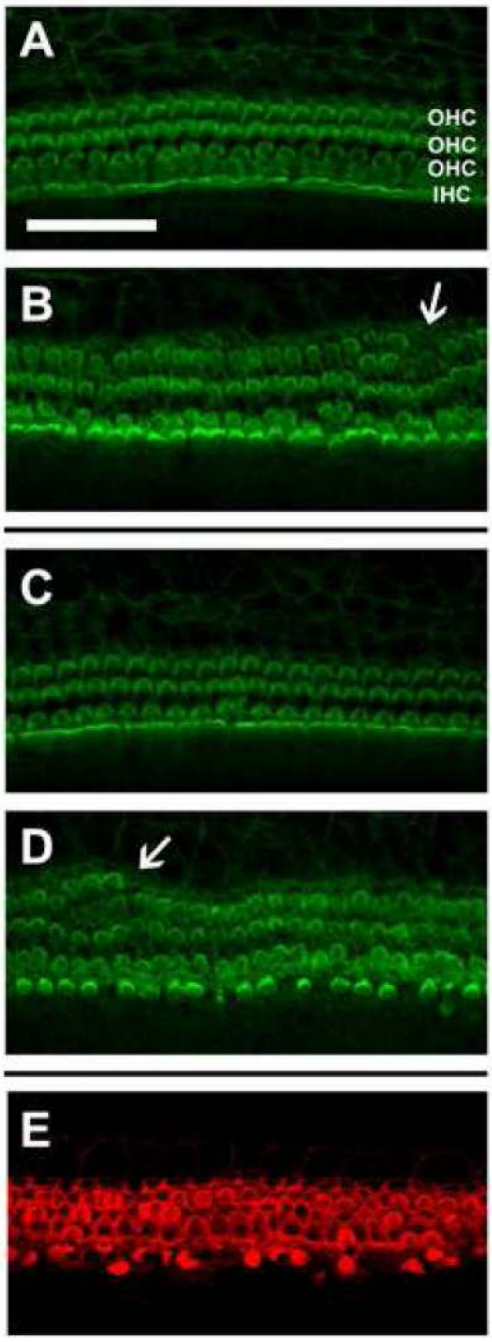

Figure 4.

Drug-induced hair cell loss in cochlear explants. Explants of the mouse organ of Corti were incubated with drugs and stained for actin as described in Experimental Section. Sections of the basal part are shown. (A) 0.1 mM compound **1**, (B) 1 mM compound **1**, (C) 0.1 mM compound **2**, (D) 1 mM compound **2** and (E) 0.2 mM gentamicin. A and C show essentially normal morphology, arrows in B and D point to small areas of missing outer hair cells, and cell loss is almost complete in E. “OHC” indicates outer, “IHC” inner hair cells. Size bar indicates the increment of 40 μm.

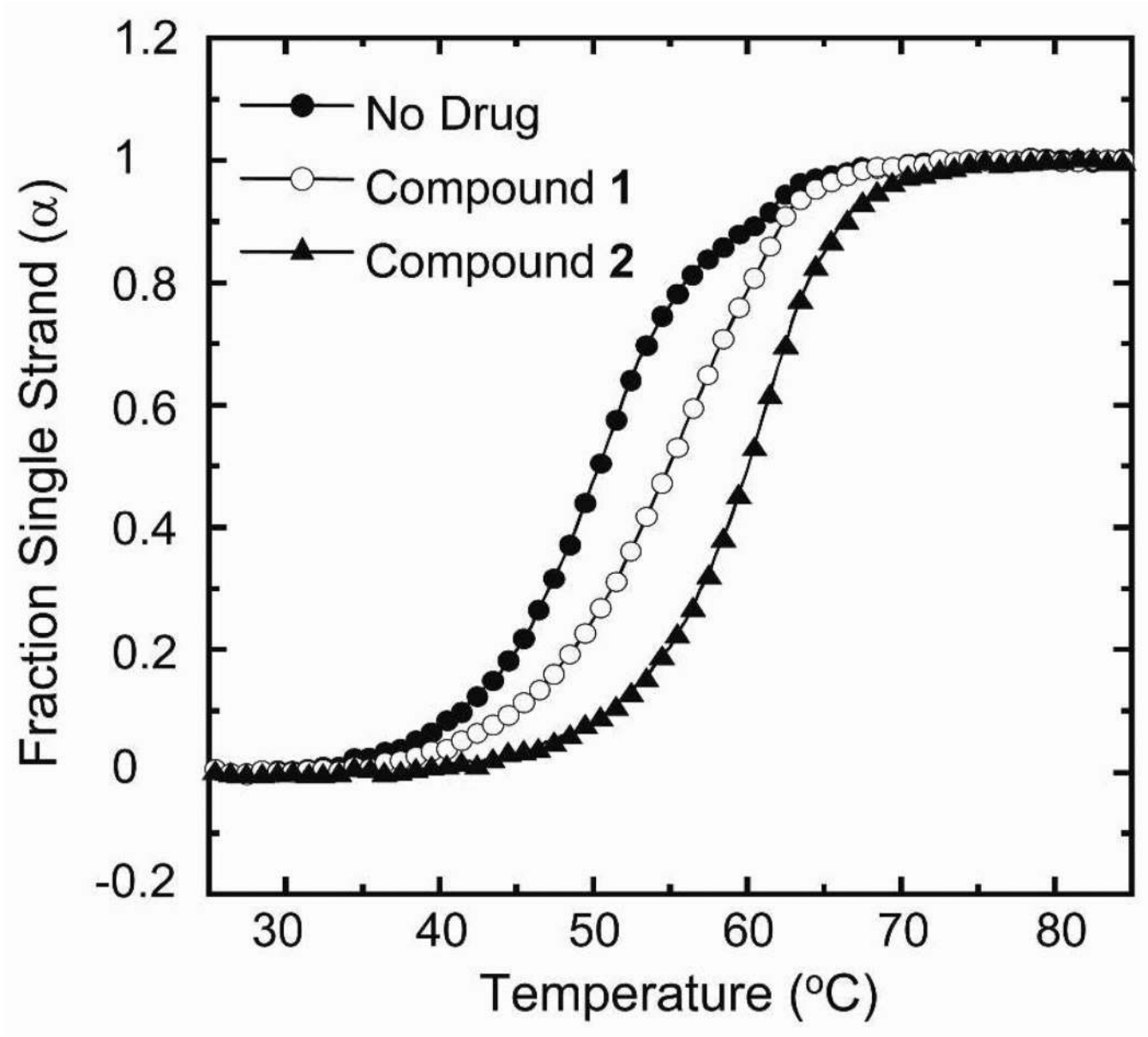

Figure 5.

UV melting profiles for a human cytoplasmic rRNA A-site model oligonucleotide in the absence (filled circles) and presence of compound **1** (open circles) and compound **2** (filled triangles) at a [drug]/[RNA] ratio of 5. For clarity of presentation, the melting curves were normalized by subtraction of the upper and lower baselines to yield plots of fraction single strand (α) versus temperature [38]. Solution conditions were 10 mM EPPS (pH 7.0) and 10 mM NaCl.

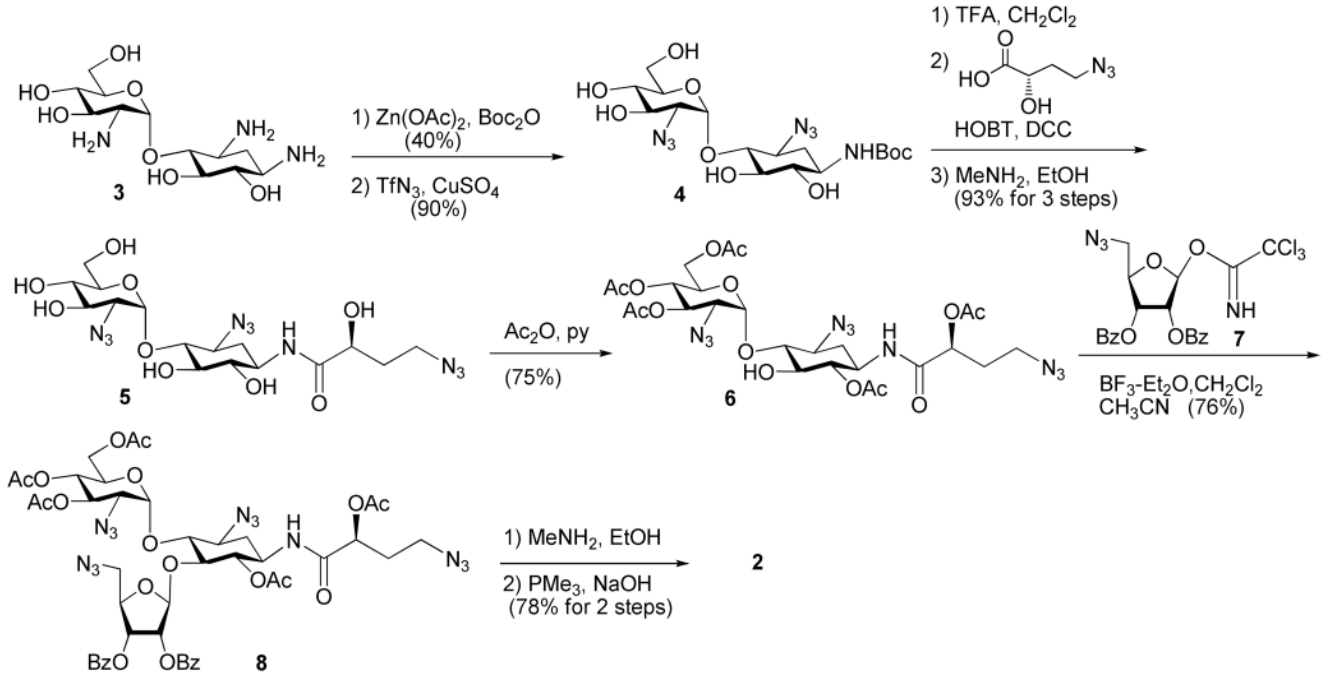

Scheme 1.
Chemical transformation of paromamine **3** into **2**.

Table 1

Comparative cell toxicity, acute intravenous toxicity, antibacterial activity and prokaryotic translation inhibition data of gentamicin, paromomycin, **1** and **2**.[a]

Aminoglycoside	Cell toxicity LC_{50} (mM)[b]			Acute toxicity	Prokaryotic system	
	HEK-293	COS-7	MDCK	LD_{50} (mg/kg)[c]	Antibacterial activity, MIC (μM)[d]	Translation inhibition, IC_{50} (nM)[e]
Gentamicin	1.1 ± 0.1	0.75 ± 0.1	0.78 ± 0.1	60	6	20 ± 6
Paromomycin	1.2 ± 0.2	1.4 ± 0.2	1.5 ± 0.1	80	22	56 ± 6
compound **1**	7.4 ± 1.4	10.8 ± 2.8	11.5 ± 1.9	240	790	415 ± 80
compound **2**	2.8 ± 0.7	9.3 ± 1.0	3.3 ± 0.3	500	588	159 ± 13

[a] In all biological tests, all tested aminoglycosides were in their sulfate salt forms. The concentrations reported refer to that of the free amine form of each aminoglycoside.

[b] Aminoglycosides-induced cell toxicity was calculated as a ratio between the number of living cells in cultures grown in the presence of the tested compound, versus cultures grown without compound. The half-maximal lethal concentration (LC_{50}) values were obtained from fitting concentration-response curves to the data of at least two independent experiments, using GraFit 5 software. HEK-293, human embryonic kidney cells; COS-7, monkey kidney cells; MDCK, canine kidney cells.

[c] LD_{50} refers to a median lethal dose.

[d] The MIC values were determined against *E. coli* R477-100 strain by using the double-microdilution method, with 384 μg/mL as starting concentration of each tested compound. All the experiments were performed in duplicates and analogous results were obtained in three different experiments.

[e] Prokaryotic translation inhibition was quantified in coupled transcription/translation assays as previously described by us[22]. The luminescence was measured immediately after the addition of 50 μl Luciferase Assay Reagent (Promega), and light emission was recorded with Victor3™ Plate Reader (Perkin-Elmer). The half-maximal concentration (IC_{50}) values were obtained from fitting concentration response curves to the data of at least two independent experiments, using GraFit 5 software.

J Med Chem. Author manuscript; available in PMC 2010 May 14.